EFFECT OF SPECIMEN SIZE ON FRACTURE TOUGHNESS IN THE DUCTILE BRITTLE TRANSITION REGION OF STEEL

D. Munz* and H. P. Keller**

***German Aerospace Research Establishment (DFVLR), Cologne, Federal Republic of Germany (now at University of Karlsruhe)**
****German Aerospace Research Establishment (DFVLR), Cologne, Federal Republic of Germany (now at TÜV Rheinland)**

ABSTRACT

Fracture mechanics tests were performed with specimens of varying thickness of a NiCrMo-steel in the ductile-brittle transition region. Below a critical thickness a transition from cleavage to dimple fracture mode was observed. It is assumed that this is caused by loss of triaxiality. The stable crack extension is less dependent on transverse constraint than unstable cleavage fracture.

KEYWORDS

Steel; ductile brittle transition; specimen size; fracture appearance.

INTRODUCTION

Determination of fracture toughness K_{Ic} requires a minimum size of the specimens. For an evaluation of the tests with linear-elastic methods the standard ASTM E 399 requires for the thickness B, the crack length a and the ligament width W-a of the specimens the same minimum value, given by

$$B,\ a,\ W\text{-}a > 2.5 \left[\frac{K_{Ic}}{\sigma_Y}\right]^2. \qquad (1)$$

It can be shown, however, that the size requirements for ligament W-a and thickness B are different. Linear elastic fracture mechanics can be applied if the plastic zone at the crack tip is small enough compared to the ligament size, leading to

$$(W\text{-}a)_{min} = \beta \left[\frac{K_{Ic}}{\sigma_Y}\right]^2. \qquad (2)$$

Experimental investigations with aluminum alloys, titanium alloys and steels, failing all in a ductile mode with a dimple structure on the fracture surface, have established $\beta = 0.4$, provided that Irwin's plastic zone correction is used for the calculation of K_{Ic} (Munz, 1979; Keller, Munz, 1977).

For the specimen thickness there exists no minimum value for the application of linear-elastic fracture mechanics. For the determination of plane strain fracture toughness K_{Ic}, however, a sufficient amount of plane strain or near plane strain

has to be present at the center of the specimen. This requirement can be written in the form

$$B_{min} = \alpha \frac{K_{Ic}^2 (1-\nu^2)}{E \sigma_y} \tag{3}$$

From theoretical and experimental investigations a value of α between 25 and 50 is suggested (Robinson, Tetelman, 1975; Munz, 1979), again for materials with ductile crack propagation.

For K_{Ic} determination with the J-integral method using three point bend or compact specimens the size requirements are (Clarke and colleagues, 1979)

$$B, W-a > 25 \frac{J_{Ic}}{\sigma_y} = 25 \frac{K_{Ic}^2 (1-\nu^2)}{E \sigma_y} \tag{4}$$

For the thickness B this requirement is identical with Eq. (3) and $\alpha = 25$.

In various investigations it was shown that for ferritic steels in the ductile-brittle transition region fracture toughness increases with decreasing specimen thickness at a critical thickness larger than given by $\alpha = 25$ (Sumpter, 1976; Hagedorn, 1980; Dahl, Zeislmair, 1978, 1980).

Two different explanations can be found in the literature for this behavior. Sumpter (1976) and Milne and Chell (1979) assume that a state of plane strain in the center of the specimen can develop only for specimens larger than given by $\alpha = 25$ and that failure by cleavage is stronger influenced by the stress state than crack propagation by void coalescence. On the other hand Landes and Shaffer (1979) explained the increase of K_{Ic} as a statistical effect, assuming a statistical variation of the local K_{Ic} along the crack front. It is assumed that crack propagation starts if at some point at the crack front the local K_{Ic} value is reached. Therefore with smaller specimens a higher average K_{Ic} is obtained than with larger specimens.

In this paper the effect of specimen thickness on the fracture behavior of a NiCrMo-steel in the ductile-brittle transition region is shown. Linear-elastic and J-integral evaluation methods were used and fracture surfaces were investigated with a scanning electron microscope.

EXPERIMENTAL PROCEDURE

The investigated material was a 4.2 % Ni - 1.68 % Cr - 0.43 % Mo steel (German designation 35 NiCrMo 16) in a normalized condition. The room temperature yield strength is 473 N/mm^2. Compact type specimens were used with a width W = 50 mm and thickness B of 25, 15, 10, 6 and 3 mm. The crack length to width ratio was 0.6. The tests were performed in the temperature range $-120\ ^{o}C \leq T \leq -80\ ^{o}C$ in a bath of isopentan, which was cooled by liquid nitrogen. Load was recorded versus load point displacement. Some specimens were unloaded before maximum load and then fatigued again. Thus the amount of stable crack growth could be seen on the fracture surface between the fatigue surfaces in the scanning electron microscope. Tensile tests were performed with specimens of 6 mm diameter.

EVALUATION PROCEDURE

For calculation of the stress intensity factor K the relation of Srawley (1976) was used. In addition the plastic zone correction was applied, replacing crack length a by

$$a^* = a + \frac{1}{6\pi}\left(\frac{K}{\sigma_y}\right)^2 \tag{5}$$

This corrected value was designated K^*.

J-integral evaluation was made according to

$$J = \frac{2\,D\,U}{B(W-a)} \tag{6}$$

where U is the area under the load - load point displacement curve and

$$D = \frac{1+\gamma}{1+\gamma^2} \tag{7}$$

with

$$\gamma = \frac{\sqrt{2}\left[1+(a/W)^2\right]^{1/2} - (1+a/W)}{1-a/W} \tag{8}$$

From J a K_J was calculated according to

$$K_J = \left[\frac{JE}{1-\nu^2}\right]^{1/2} \tag{9}$$

The room temperature value E = 207 200 N/mm^2 and ν = 0.3 were used for all temperatures.

The values determined at maximum load are designated K_{max}, K^*_{max}, J_{max} and K_{Jmax}. In addition the 5 % secant method was used for the evaluation of K_Q.

RESULTS

Yield strength and ultimate tensile strength are shown in Fig. 1.
The general behavior of the load -load point displacement curve is plotted in Fig. 2.

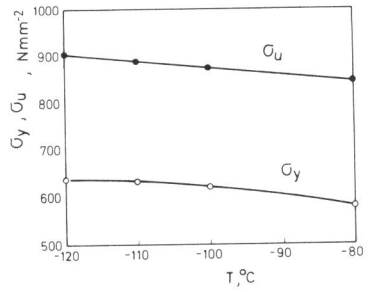

Fig. 1. Yield strength σ_y and ultimate strength σ_u vs. temperature

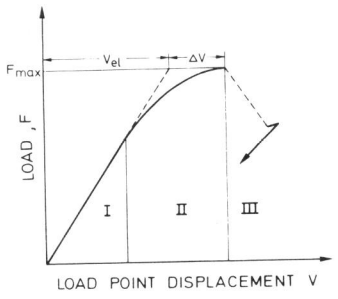

Fig. 2. Load vs. load point displacement (schematic)

After a linear region I a deviation from linearity is observed in region II, which can be caused by plastic deformation or stable crack extension. After reaching maximum load F_{max} a sudden drop in the load and an increase in the displacement caused by rapid crack extension occurred (region III). Dependent on temperature and specimen thickness the specimen fractures completely or the crack arrests after some load drop. Then the specimen was unloaded and fatigued again.

In Fig. 3 typical load - load point displacement curves are plotted for specimens with thicknesses of 25, 6 and 3 mm. The different slopes in region I are due to different initial crack lengths. Generally the nonlinear displacement Δv at maximum load increases with decreasing thickness and increasing temperature. There was, however, some scatter in the displacement at maximum load, especially at -80 °C. For the specimens with B = 25 mm the deviation from linearity is small below -80 °C. For the specimens with B = 6 mm and B = 3 mm the deviation is small only below -100 °C.

K_Q and K_{max} (average values of 2 to 5 tests) are plotted against temperature in Fig. 4. It can be seen that there is a larger increase in K_{max} than in K_Q with temperature. In Fig. 5 K^*_{max} is plotted against thickness for the different temperatures. In the range -120 °C $\leq T \leq$ -90 °C K^*_{max} is independent of thickness above a critical thickness B_{min}. For $B < B_{min}$ K^*_{max} increases. Only for -80 °C does there seem to be a minimum at B = 10 mm.

In Fig. 6 K_{Jmax}, the stress intensity factor calculated from J-integral at maximum load, is plotted against thickness. K_{Jmax} is also constant above a critical thickness, which is , however, larger than for K^*_{max}. In Fig. 7 K_{Jmax} is plotted against K^*_{max}. K_{Jmax} exceeds K_{max} for $K_{max} > 110$ $MNm^{-3/2}$, i.e. for specimens tested at -80 °C and for the thinner specimens tested at -90 °C and -100 °C.

The fracture appearance is dependent on testing temperature and specimen thickness and shows the same feature as described by Milne and Chell (1979). The description is made separately for the different temperatures.

-120 °C and -110 °C: In the range 6 mm $\leq$ B $\leq$ 25 mm first a stretched zone and then a region with mainly cleavage structure was found adjoining the fatigue crack (Fig. 8a). There are only some isolated dimple regions. Only for the specimens with B = 3 mm (Fig. 8b) did a mixed dimple/cleavage region precede the pure cleavage region. The extension of this region averaged along the crack front was between 90 µm and 160 µm for the tests at -120 °C and about 200 µm for the tests at -110 °C.

-100 °C: In the range 10 mm $\leq$ B $\leq$ 25 mm regions with dimples could be seen adjoining the stretched zone (Fig. 9). These regions sometimes were isolated. Averaged along the crack front extension of the dimple region was 40 µm or less. The specimens with B = 6 mm and B = 3 mm had a much larger mixed dimple/cleavage region up to 200 µm before pure cleavage fracture occurred.

-90 °C: For the specimens with 10 mm $\leq$ B $\leq$ 25 mm the region was less than 70 µm. Only for one specimen with B = 25 mm the extension of the dimple/cleavage structure was 450 µm. For all specimens with B = 3 mm and B = 6 mm the region containing dimples was larger than 200 µm.

-80 °C: All specimens had a well developed dimple region before cleavage (Fig. 10). The extension of this region showed a large amount of scatter, for instance for specimens with B = 15 mm between 58 µm and 750 µm.

By unloading before maximum load it could be shown that the mixed dimple/cleavage fracture appearance developed in region II of Fig. 2 and is therefore characteristic of the stable crack extension. The pure cleavage fracture surface is

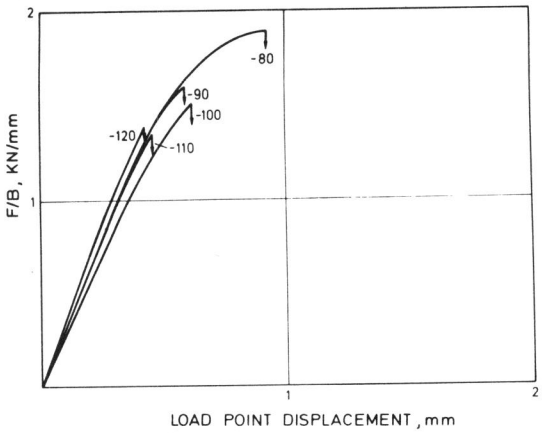

B = 25 mm

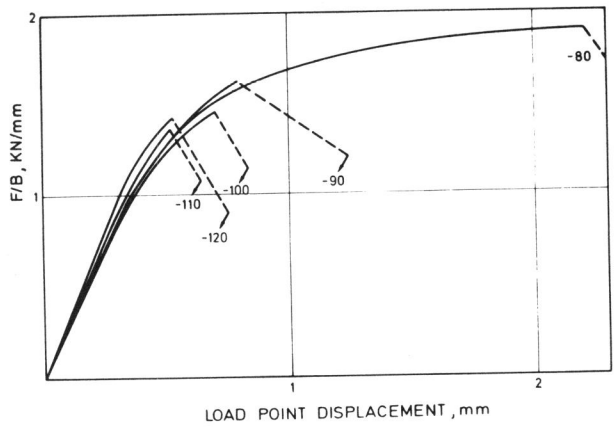

B = 6 mm

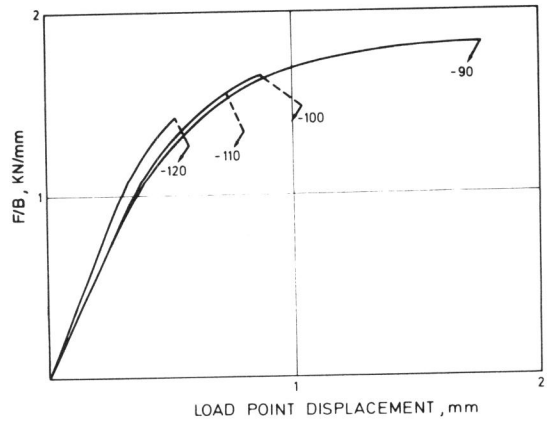

B = 3 mm

Fig. 3. Load devided by thickness v. load point displacement.

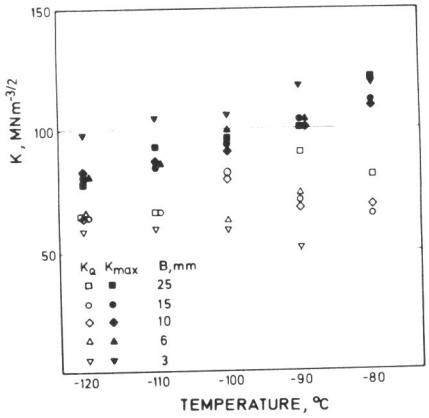

Fig. 4. K_Q and K_{max} vs. temperature

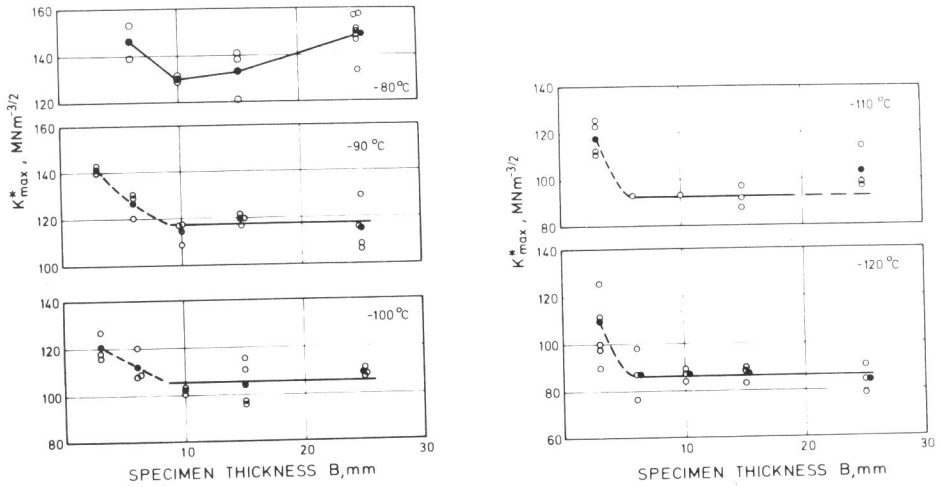

Fig. 5. K^*_{max} vs. specimen thickness
(open symbols: individual results; filled symbols: average values)

characteristic of the unstable crack extension in region III.

J - Δa and K* - Δa - curves are shown in Fig. 11 and 12. The open symbols are for specimens unloaded before maximum load, the filled symbols for specimens with unstable crack extension, where Δa is the stable crack extension up to maximum load.

In Fig. 11 J - Δa - curves are plotted for -80 °C and -90 °C. For -80 °C the points are within a scatter band with the exception of the specimens with B = 6 mm. The stretched zone was not included in the Δa - determination, therefore no blunting

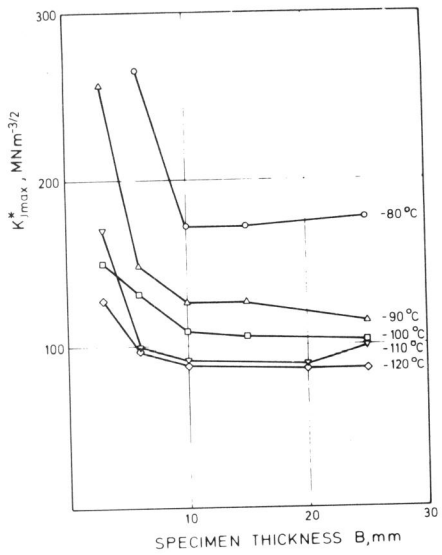

Fig. 6. K_{Jmax} vs. specimen thickness

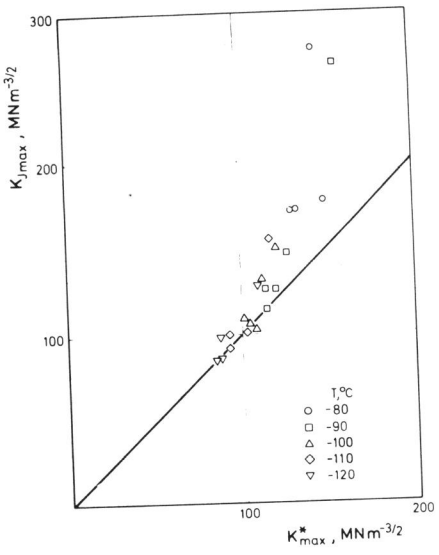

Fig. 7. K_{Jmax} vs. K^*_{max}

line was drawn in the figures. The curve at -80°C is steep at small crack extensions and extrapolation to zero crack extension is difficult. An extrapolation to Δa = 0.1 mm is easier. For the specimens with 10 mm ≤ B ≤ 25 mm a straight line can be drawn, leading to $J_{0.1}$ = 106 N/mm and $K_{J0.1}$ = 155 MNm$^{-3/2}$. The curve for B = 6 mm is steeper, however, $J_{0.1}$ is about the same as for the larger specimens. For the tests at -90 °C $J_{0.1}$ = 100 N/mm and $K_{J0.1}$ = 151 MNm$^{-3/2}$ is obtained from Fig. 11.

Fig. 12 shows as an example a K* - Δa - curve for -90 °C. From this figure and similar ones for the other temperatures $K_{0.1}$ at Δa = 0.1 mm was obtained and plotted against temperature (Fig. 13). K^*_{max} and K_{Jmax}, also plotted in Fig. 13, are the thickness-independent values for B > B_{min} . At T ≤ 90 °C most of the specimens especially the thicker ones failed before reaching 0.1 mm crack extension. Therefore there is $K^*_{max} < K^*_{0.1}$, whereas at -80 °C instability starts at larger crack extensions and therefore there is $K^*_{max} > K^*_{0.1}$.

DISCUSSION

For the evaluation of the results linear-elastic methods and J-integral were used. In the introduction it was mentioned that K_J from J-integral and K* from linear elastic evaluation with plastic zone correction should be identical for $\beta > 0.4$ (see Eq. (1)). The β-values calculated from K^*_{max}, σ_y and W-a = 20 mm are given in Table 1 for the smallest and the largest specimens of each temperature. It can be seen that there is $\beta > 0.4$ for T ≤ -90 °C with the exception of B = 3 mm for T = -90 °C. For T = -80 °C β is somewhat below 0.4. Therefore at least for T ≤ -90 °C K^*_{max} should be the correctly evaluated stress intensity factor. There is in fact a good agreement between K^*_{max} and K_{Jmax}, if no stable crack extension occurs before maximum load. The stable crack extension affects K_J more than K*, because of the change in compliance. This can be seen from Fig. 14, where K_J and K* are plotted

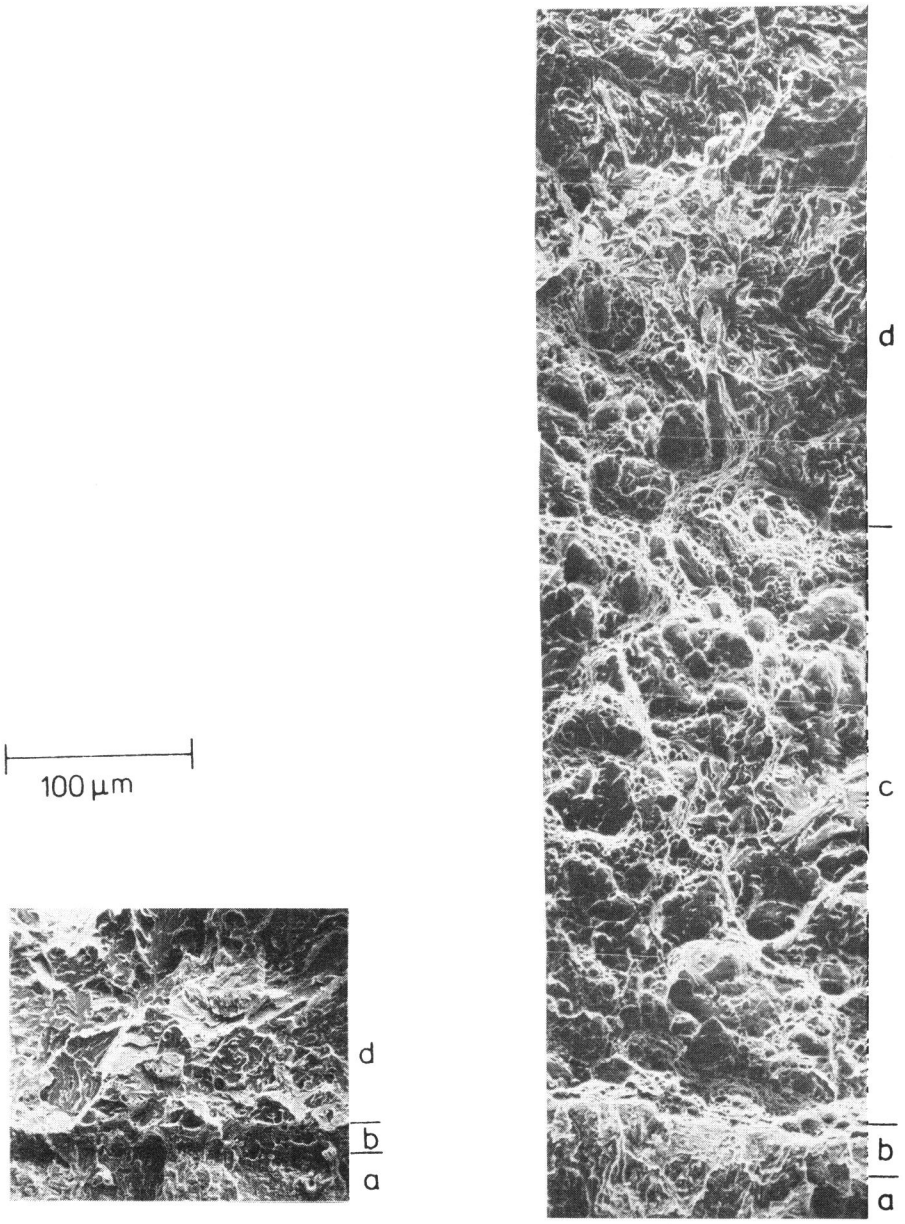

a
B = 6 mm

b
B = 3 mm

Fig. 8. Fracture surfaces of specimens fractured at -120°C (a fatigue crack, b stretched zone, c stable crack extension, d unstable crack extension)

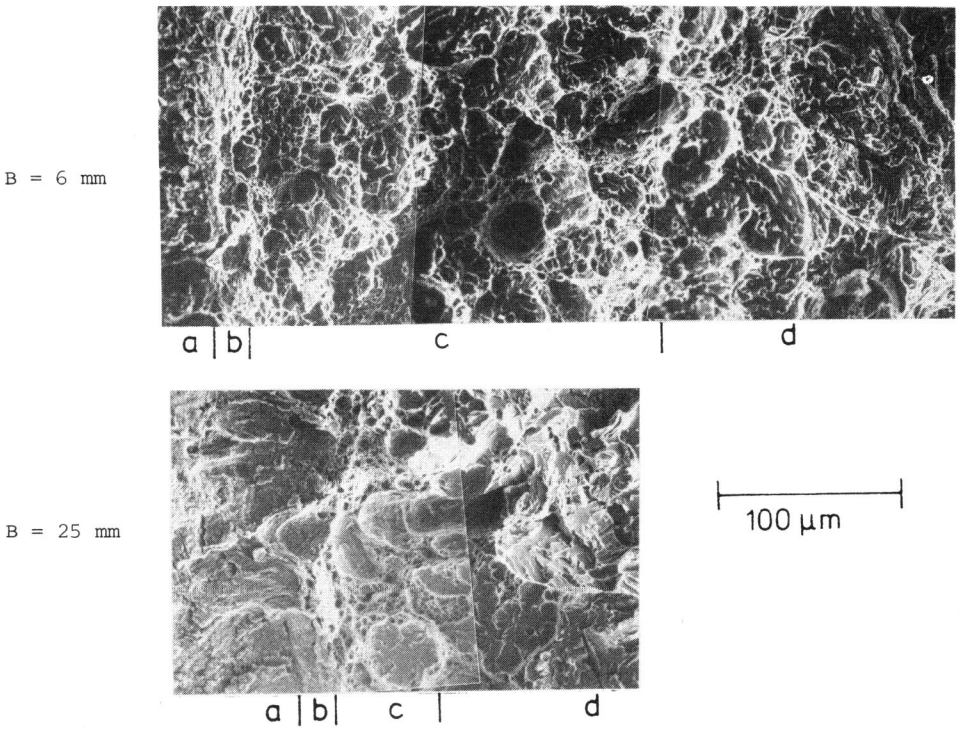

Fig. 9. Fracture surfaces of specimens fractured at -100°C

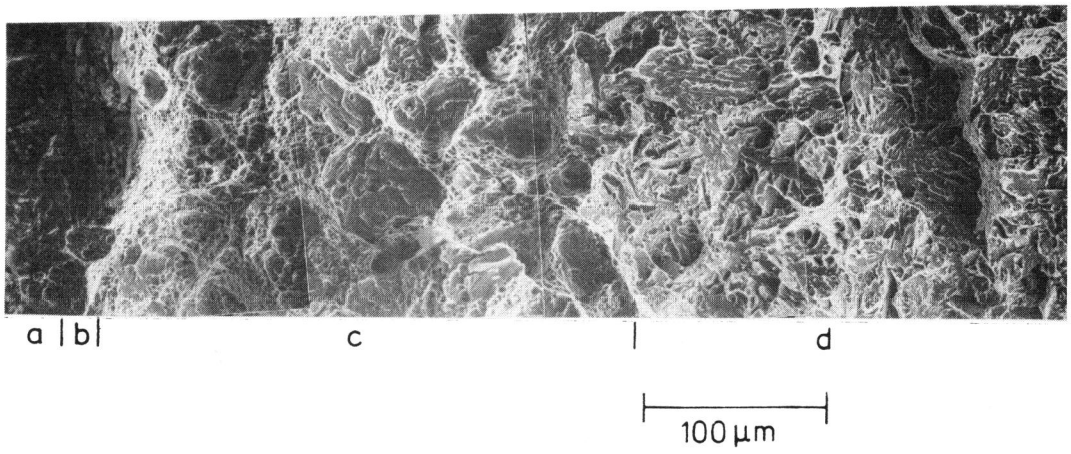

Fig. 10. Fracture surface of a specimen with B = 15 mm fractured at -80°C

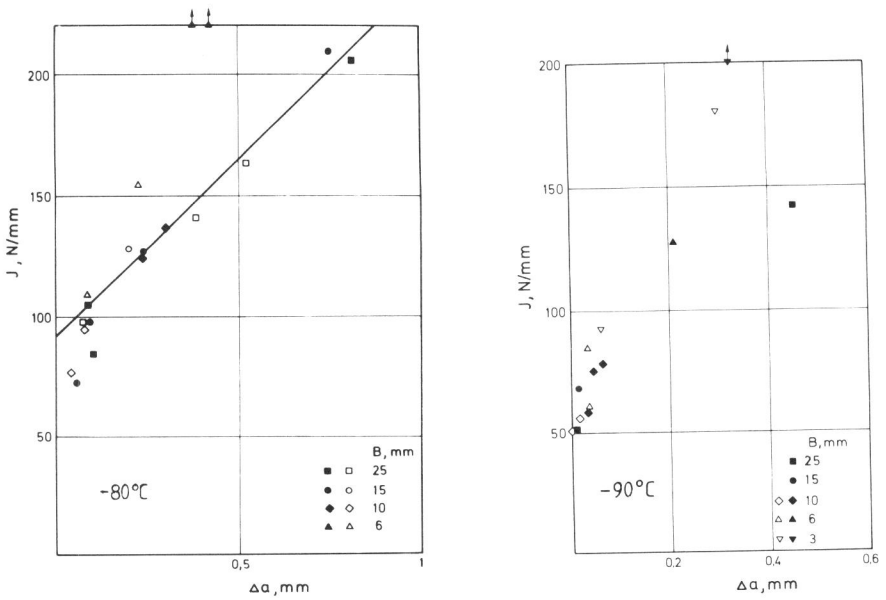

Fig. 11. J - Δa - curves for -80 °C and -90 °C

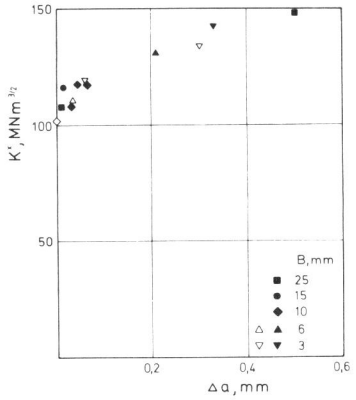

Fig. 12. K* - Δa - curve for -90 °C

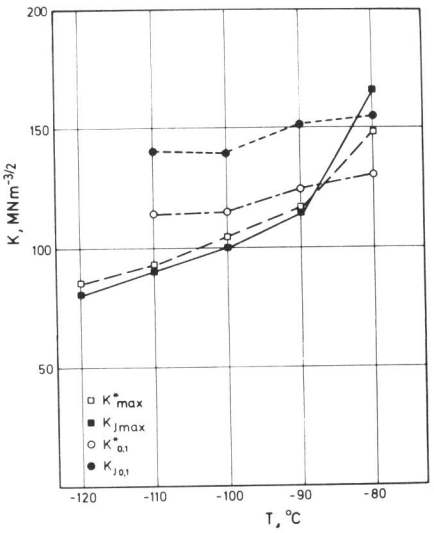

Fig. 13. Different K-values vs. temperature

TABLE 1 β According to Eq. (2)

Temp. °C	σ_y N/mm^2	B mm	K^*_{max} MNm$^{-3/2}$	β
-80	581	25	148.5	0.31
		6	146	0.32
-90	604	25	114.5	0.56
		3	141.4	0.36
-100	621	25	108.0	0.66
		3	120.5	0.53
-110	632	25	103.0	0.75
		3	117.8	0.58
-120	637	25	84.1	1.15
		3	110.1	0.67

against Δa for the tests at -80 °C. With increasing crack extension the difference between K_J and K* increases.

At all temperatures and for all thicknesses unstable fracture with a cleavage fracture appearance occurred. Above critical thickness B_{min} no or only a very small amount of stable crack extension with a dimple fracture appearance preceded the unstable fracture. K^*_{max} is constant for $B > B_{min}$. For $B < B_{min}$ cleavage fracture is preceded by stable crack extension in a mixed dimple/cleavage mode and K^*_{max} is larger than in the thickness-independent region.

It is assumed that the transition from cleavage to dimple fracture is caused by the stress state at the crack tip. In the schematic Fig. 15 stress intensity factors

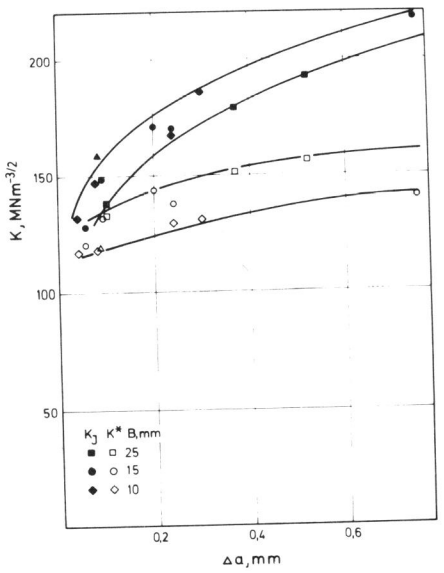

Fig. 14. K_J and K* vs. crack extension at -80 °C

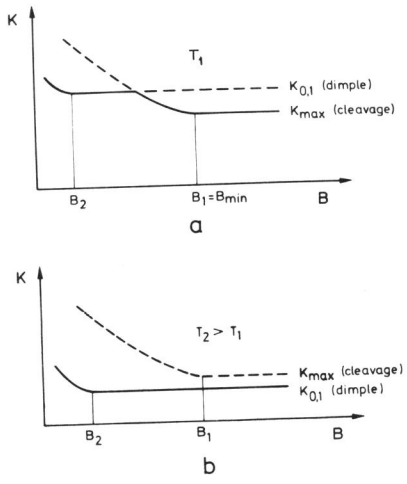

Fig. 15. K_{max} at the onset of unstable cleavage fracture and $K_{0.1}$ at the onset of stable crack growth

are plotted against thickness B. For a given temperature there are two critical stress intensity factors characterizing the fracture behavior under plane strain conditions, one for brittle cleavage fracture and the other for ductile crack extension with dimple formation. At the onset of cleavage fracture the load drops suddenly, therefore the critical K-value is K_{max}. For ductile crack extension the stress intensity factor increases with crack extension. In Fig. 15 the value at the beginning of crack extension $K_{0.1}$ is plotted. Below a critical thickness B_{min} K_{max} increases because of the loss of constraint. For thin enough specimens the critical stress intensity factor for dimple formation ($K_{0.1}$) is reached before cleavage fracture can occur. Then stable crack extension precedes unstable cleavage fracture. The critical thickness for the development of a plane strain state at the specimen center is given by α in Eq. (3). From Table 2 a value of about 100 is suggested for α. This value will be called α_1 in the following.

TABLE 2 α According to Eq. (3)

Temp. °C	B_{min} mm	$R_{p0.2}$ Nmm^{-2}	K^*_{max} $MNM^{-3/2}$	α
-120	<6	637	86	<118
-110	<6	632	92	<102
-100	<10	621	105	<128
-90	<10	604	116	<102

Whereas the onset of unstable fracture seems to be strongly dependent on thickness and therefore on stress state, the stable crack extension characterized by the J - Δa - curve or the K*- Δa - curve is less affected by thickness. It is therefore assumed that the stable crack extension with a mixed dimple/cleavage fracture mode is less dependent on the stress state. The J - Δa - and the K* - Δa - curves therefore are the plane strain crack growth resistance curves, even if there is some through the thickness deformation. Therefore $K_{0.1}$ is independent of thickness also below α_1. If thickness and triaxiality are further reduced and a more plane stress state occurs, $K_{0.1}$ also should increase. The critical thickness is called B_2 in Fig. 15. The corresponding α_2 is the critical value for ductile crack extension and should be 25 according to J-integral experience.

The critical value α_1 = 100 obtained in the present investigation can be compared with results in the literature. Chell and Worthington (1976) also found for a MnCrMo-steel a transition from cleavage to dimple fracture if the thickness is reduced. For specimens with B = 25 mm cleavage and for specimens with B = 15 mm slow crack growth was found. From K^*_{max} and σ_y α_1 < 120 was calculated in good agreement with the results in this investigation. Keller (1979) found a transition from cleavage to dimple fracture for the steel StE47 at -50°C below B = 15 mm, from which α_1 < 155 is calculated. From investigations of Dahl and Zeislmair (1980) for the same steel it can be concluded that α_1 increases with decreasing temperature. Hagedorn (1980) investigated different steels and found an increase in K_{max} at thicknesses much larger than given by α = 100.

On looking over these results there still remains some confusion. While some results can be sufficiently described by Fig. 15 with α_1 = 100, higher values of α are obtained for some others. Further investigations are yet necessary to find out general rules to describe the fracture behavior in the ductile-brittle transition region.

CONCLUSIONS

Fracture mechanics tests were performed with compact specimens of varying thickness B of a NiCrMo-steel in the ductile-brittle transition region. The following results and conclusions were obtained:

1. For $-120^{\circ} < T < -90^{\circ}C$ the stress intensity factor at maximum load is constant for $B > B_{min}$ and increases for $B < B_{min}$. The critical thickness B_{min} increases with temperature.

2. For $B < B_{min}$ stable crack extension with a mixed dimple/cleavage fracture appearance preceded the unstable cleavage fracture. For $B > B_{min}$ no stable crack extension was observed and cleavage fracture was found adjoining the stretched zone. At $-80^{\circ}C$ stable crack growth preceded unstable fracture at all investigated thicknesses.

3. It is assumed that the transition from cleavage to dimple fracture mode is caused by a loss of triaxiality. The critical thickness corresponds to $\alpha_1 = 100$ in eq. (3). The stable crack extension is less dependent on triaxiality and therefore a plane-strain stable crack growth resistance curve can be obtained with thinner specimens.

ACKNOWLEDGEMENT

The financial support of the Deutsche Forschungsgemeinschaft is gratefully acknowledged.

REFERENCES

Chell, G.G., and P.J. Worthington (1976). Mat. Sci. & Eng., 26, 95-103.
Clark, G.A., W.R. Andrews, J.A. Begley, J.K. Donald, G.T. Embley, J.D. Landes, D.E. McCabe, and J.H. Underwood (1979). J. Test. & Eval., 7, 49-56.
Dahl, W., and H.C. Zeislmair (1978). Fortschritt-Berichte der VDI Zeitschriften Reihe 18, Nr.6 (Proceedings Second European Colloquium on Fracture), 170-177.
Dahl, W., and H.C. Zeislmaier (1980). Archiv für Eisenhüttenwesen, 51, 7-14.
Hagedorn, K.E. (1980). Archiv für Eisenhüttenwesen, 51, 15-20.
Keller, H.P. (1979). Report DFVLR-FB79-03 of the German Aerospace Research Establishment.
Keller, H.P., and D. Munz (1977). Flaw Growth and Fracture, ASTM STP 631, 217-231.
Landes, J.D., and D.H. Shaffer (1979). Westinghouse Scientific Paper 79-1D3-JINTF-P4.
Milne, I., and G.G. Chell (1979). Elastic-Plastic Fracture, ASTM STP 668, 358-377.
Munz, D. (1979). Elastic-Plastic Fracture, ASTM STP 668, 406-425.
Munz, D. (1979). Report DFVLR-FB79-31 of the German Aerospace Research Establishment.
Robinson, J.N., and A.S. Tetelman (1975). Int. J. Fract., 11, 453-468.
Srawley, J.E. (1976). Int. J. Fract., 12, 475-476.
Sumpter, J.D.G. (1976). Metal Science, 10, 354-356.